Pediatric Cardiovascular CT Angiography: Radiation Dose Reduction Using Automatic Anatomic Tube Current Modulation

Christopher Herzog[1]
Denise M. Mulvihill[1]
Shaun A. Nguyen[1]
Giancarlo Savino[1]
Bernhard Schmidt[2]
Philip Costello[1]
Thomas J. Vogl[3]
U. Joseph Schoepf[1]

Herzog C, Mulvihill DM, Nguyen SA, et al.

OBJECTIVE. The purpose of this study was to assess the effect of weight-based scanning protocols and automatic tube current modulation on the tube current–time product and image quality at pediatric cardiovascular 64-MDCT angiography.

MATERIALS AND METHODS. Our pediatric cardiovascular 64-MDCT protocols use a weight-based algorithm to determine nominal tube voltage settings with 80, 100, and 120 kV. Automatic tube current modulation was used for each case. The mAs, volume CT dose index ($CTDI_{vol}$), and dose–length product (DLP) values were recorded and the effective dose calculated. On the basis of the selected nominal tube current, the dose values that would have been delivered without tube current modulation were also calculated. Scans were compared with 16-MDCT using 120 kVp and 120 mAs. Two radiologists independently rated image quality on a 5-point scale. Image noise was objectively measured within four different regions of interest. Findings at CT were clinically correlated with results of cardiac sonography, angiography, or surgery.

RESULTS. Thirty-eight 64-MDCT and 30 16-MDCT scans were evaluated. Mean diagnostic quality for 64-MDCT was rated at 3.6 ± 0.4 (SD) and mean image noise was 8.9 ± 4.5 H. Results with 16-MDCT were not significantly different: diagnostic quality (3.6 ± 0.4; $p = 0.97$) and image noise (9.1 ± 2.8 H; $p = 0.31$). Scanning with automatic tube current modulation significantly ($p < 0.05$) reduced the tube current time–product compared with scanning without automatic tube current modulation (–57.8% / 54.1 / 128 mAs) or with 16-MDCT (–47.9% / 54.1 / 104.37 mAs), respectively. The mAs values were significantly ($p < 0.05$) lower for 80 kVp than for 100 or 120 kVp scans, but image quality and image noise were not significantly ($p = 0.24$) different. Agreement between MDCT and clinical findings was excellent.

CONCLUSION. Under simulated conditions, automatic tube current modulation combined with low tube voltage settings significantly reduced radiation exposure and thus appears preferable in pediatric cardiovascular 64-MDCT.

Keywords: congenital abnormalities of the chest, CT image quality, CT in infants and children, CT radiation exposure, CT technology

DOI:10.2214/AJR.07.3124

Received January 16, 2007; accepted after revision November 9, 2007.

B. Schmidt is an employee of Siemens Medical Solutions. U. J. Schoepf is a medical consultant to Siemens Medical Solutions and GE Healthcare and receives research support from Siemens, GE, and Medrad. Authors of this article who are not employees of Siemens Medical Solutions had control of inclusion of any data and information that might present a conflict of interest for those authors who are employees of that industry.

Presented at the 2007 annual meeting of the Radiological Society of North America, Chicago, IL.

[1]Department of Radiology, Medical University of South Carolina, 169 Ashley Ave., Charleston, SC 29425. Address correspondence to U. J. Schoepf (schoepf@musc.edu).

[2]Siemens Medical Solutions, Forchheim, Germany.

[3]Department of Radiology, Johann Wolfgang Goethe University, Frankfurt, Germany.

AJR 2008; 190:1–9

0361–803X/08/1905–1

AQ-1

The National Academy of Sciences recently released a report stating that even low doses of ionizing radiation are likely to pose some risk of adverse health effects [1]. Exposure to radiation is of special concern in children because of the greater vulnerability to radiation effects of this population compared with adults [2, 3]. Because of the evident advantages of MDCT, most notably scanning speed obviating sedation, the number of CT examinations in children is rapidly increasing. Whereas in 1993 only 6% of CT examinations were performed in children [3], currently the percentage has increased to approximately 10%, delivering about 67% of the overall collective radiation dose to this population [4].

At the same time, only 43% of institutions adjust their CT techniques when examining children [5]. Several authors have recommended reducing the tube current–time product or the tube potential or both as a function of patient size, with the goal of obtaining constant diagnostic quality and image noise at reduced radiation [6–8]. However, selecting a tube current that will yield acceptable image quality with the lowest possible radiation is still challenging. Automatic anatomic tube current modulation represents a recent development to optimize radiation dose [9]. With this technology, the tube current is constantly adjusted to the patient's anatomy so that consistent image quality is achieved throughout the body. First clinical studies show up to 66% radiation reduction without compromising image quality [9–11].

The aim of this study was to assess the effect of weight-based scanning protocols and

automatic tube current modulation in children with congenital thoracic cardiovascular abnormalities and to compare the 64-MDCT angiography results with the results of cardiac sonography, angiography, or surgery.

Materials and Methods

Subject Demographics

Our institutional human research committee approved the retrospective evaluation of patient MDCT data. The need for informed patient consent was waived. In compliance with HIPAA regulations, all identifying information was removed by deleting all patient-related data from DICOM headers and clinical charts before evaluation.

The MDCT data sets of 68 consecutive pediatric patients (41 male, 27 female) referred to our department between July 2003 and April 2005 for known or suspected congenital cardiovascular anomalies of the thorax were evaluated. In all patients, the weight was recorded.

Of the 68 patients, 38 underwent 64-MDCT and 30 underwent 16-MDCT. The 64-MDCT, patients were divided into three groups: 80 kVp (n = 17), 100 kVp (n = 9), and 120 kVp (n = 12). A normality distribution test (Kolmogorov-Smirnov) was determined according to the following variables for all three groups: age, height, and body weight. Variables had Kolmogorov-Smirnov distribution between 0.073 and 0.126 ($p > 0.20$). The mean age of our consecutive cohort of 38 patients who underwent 64-MDCT with automatic tube current modulation was 5.8 years (age range, 1 day–15 years). Mean height was 100.4 cm (range, 45.1–173 cm), and mean body weight was 21.9 kg (range, 2.3–74.2 kg). Similar variables were observed for the 30 patients who underwent 16-MDCT. Table 1 summarizes patient demographics for both patient populations.

Of the 38 patients (21 males, 17 females), who underwent 64-MDCT with automatic tube current modulation, 16 were scanned for postoperative follow-up and 22 had no history of surgery. In the 30 patients (14 males, 16 females) who underwent 16-MDCT, the ratio was 18 and 12, respectively. Table 1 summarizes all cardiovascular defects of all patients enrolled in this study.

AQ-2

Image Acquisition

In 38 patients, scanning was performed on a 64-MDCT scanner (SOMATOM Sensation 64 Cardiac, Siemens Medical Solutions). Scanning parameters were 64 × 0.6 mm collimation, z-flying focal spot technique [12], 0.33-second rotation time, and pitch of 1.5. According to previously published work [13–16], the tube voltage was individually adjusted to patient weight: Patients weighing < 15 kg were scanned at 80 kVp (n = 17); patients weighing ≥ 15 kg were scanned at either 100 kVp (n = 9) or 120 kVp (n = 12) [15, 16] at the discretion of the physician prescribing the scanning parameters (some radiologists routinely prescribed 100 kVp and some 120 kVp). All 38 patients were scanned using commercially available tube current modulation software (CAREDose4D, Siemens Medical Solutions). This software affords online monitoring of tissue attenuation and real-time adjustment (i.e., z-modulation) of the base tube current as a function of the projection angle, with a delay of 360° [17, 18]. The base tube current was set at 72 mAs. For projections with low attenuation, the maximal reduction of the tube current is 90%. For

TABLE 1: Patient Demographics

Parameter	64-MDCT With Automatic Anatomic Tube Current Modulation (AATCM)								16-MDCT Without AATCM	
	80 kVp		100 kVp		120 kVp		Mean		120 kVp	
	Mean	Range	Mean	Range	Mean	Range	Mean	Range	Mean	Range
Age	0.6 y	1 d–4 y	8.5 y	4 m–13 y	9.2 y	5 m–15 y	5.8 y	1 d–15 y	6.0 y	1 d–15 y
Height (cm)	61.6	45.2–101	123.9	69.3–156	124.9	52.3–173	100.4	45.2–173	104.0	44.7–184
Weight (kg)	4.8	2.3–8.5	31.8	15.5–54.1	32.9	16.3–74.2	21.9	2.3–74.2	25.8	2.0–87.6
Main cardiovascular defects[a]										
Aortic coarctation					10				7	
Aortic ring or right aortic arch					11				7	
Tetralogy of Fallot					5				5	
Abnormal pulmonary vein drainage					9				5	
Pulmonary artery stenosis					7				3	
Arterial septal defect					6				4	
Transposition of great vessels					1				1	
Pentalogy of Cantrell					1				NA	
Subvalvular aortic stenosis					5				1	
Ebstein's anomaly					2				NA	
Takayasu's arteritis					1				NA	
Klippel-Trénaunay-Weber syndrome					1				NA	
Heterotaxy or malposition					NA				1	
Truncus arteriosus					NA				1	
Single ventricle					NA				1	
Total					59				36	

Note—NA indicates not available.
[a]Several patients had more than one anomaly.

each acquisition, the CT unit calculates the arithmetic mean mAs_{eff} throughout the exposure. Mean scanning time was 4.3 seconds (range, 3.2–6.8 seconds).

In 30 patients, scanning was performed on a 16-MDCT scanner (LightSpeed, GE Healthcare). Scanning parameters were 16 × 0.625 mm collimation, 0.5-second rotation time, pitch of 1.5, 120-kVp tube voltage, and a weight-adapted tube current ranging between 32 and 110 mAs. Reference mAs values for different weight groups have been previously published elsewhere [7]. Mean scanning time was 10.4 seconds (range, 7.3–14.7 seconds).

In all 68 patients, the scanning range extended from the thoracic outlet to just below the diaphragm. All examinations were performed after IV administration of 2 mL/kg of body weight of 300 mg I/mL of iohexol (Omnipaque 300, GE Healthcare) diluted 2:1 with 0.9% saline. In 44 patients (16-MDCT, 17 patients; 64-MDCT, 27 patients), contrast material was injected using an automated power injector (Stellant D, Medrad). Scanning delay time was determined by the automated bolus triggering technique, using a threshold of 160 H as detected within a region of interest (ROI) placed either in the pulmonary trunk or in the ascending aorta, depending on the clinical indication (Table 1). In 24 newborns (16-MDCT, 13 patients; 64-MDCT, 11 patients) bolus triggering was not possible and contrast material was injected manually. In these cases, the start delay for CT was adjusted to the target vessel: Scanning of the pulmonary arteries, right atrium, and right ventricle was commenced after injection of two thirds of the contrast and saline solution; scanning of the pulmonary veins, left atrium, left ventricle, and aorta began after injection of three quarters of the solution. Retrospective ECG gating was not used in this cohort. Thirty-three patients were scanned in inspiratory breath-hold (16-MDCT, 15 patients; 64-MDCT, 18 patients). Thirty-seven patients—particularly newborns and younger children—were scanned using the free-breathing technique to avoid the need for intubation or sedation (16-MDCT, 15 patients; 64-MDCT, 22 patients).

For image reconstruction, an individually adapted field of view, a matrix size of 512 × 512 pixels, and a soft-tissue convolution kernel (B25f) were used. Images were reconstructed as 0.75- and 3-mm thick sections with an increment of 0.4 and 3 mm, respectively.

AQ3

Image Analysis

Image evaluation was performed on a standard 3D-enabled workstation (Leonardo, Siemens Medical Solutions) with a standardized window level of 100 H and window width of 700 H. Each subject was analyzed independently by a cardiovascular radiologist and a pediatric radiologist, with 6 and 12 years, respectively, of professional experience. Both observers were aware of the clinical data—as a prerequisite for the assessment of complex cardiovascular defects—but were blinded to the scanning parameters and patient characteristics (weight, age, sex).

Each data set was assessed for image noise and graded for image quality. In accordance with previous publications [19–21], image noise was determined on 3-mm transverse sections by measuring the SD [19] in Hounsfield units within four ROIs (> 100 pixels) consistently placed in the descending aorta at the level of the right pulmonary artery, the trachea just above the bifurcation, the pulmonary artery, and the right greater pectoralis muscle [20, 21]. The average noise value (SD) of the four ROI measurements was calculated for each subject and expressed as mean ± SD.

To assess diagnostic image quality, both readers were asked to independently assess the display of relevant vascular structures and to identify any cardiovascular defects. Relevant vascular structures included the heart (i.e., both ventricles and atria, myocardium, septum, cardiac valves, and the ostia of the left and right coronary arteries), the thoracic aorta, the supraaortic branches, and the pulmonary arteries and veins. Image quality was graded using previously published criteria [10, 22, 23]: Criteria for image quality were the subjective perception of image noise, soft-tissue contrast, sharpness of tissue interfaces, conspicuity of anatomic detail, and degree of image degradation by streak or beam-hardening artifacts. All structures were assessed using a 5-point scale: A score of 1 for unacceptable, 2 for suboptimal, 3 for adequate, 4 for good, and 5 for excellent diagnostic quality. On the basis of the individual scores for relevant vascular structures and anatomic anomalies, an average quality score was calculated for each patient. Diagnostic quality was considered sufficient when the mean score was rated 3 or higher [10, 22, 23].

Finally, all cardiovascular defects that had been documented on MDCT scans were compared with cardiac sonography and either catheter angiography or surgery.

Estimation of Radiation Dose

In the 38 patients who underwent 64-MDCT and the 30 patients who underwent 16-MDCT, respectively, the tube current–time product (mAs), tube voltage (kVp), scan length (mm), scanning time (seconds), table feed per rotation (mm), and total collimation ($n \times h_{vol}$) were recorded and used as input parameters for commercially available CT dose calculation software (CT-Expo version 1.5, G. Stamm and H. D. Nagel). The software uses pediatric CT reference values that have been previously described elsewhere [24, 25]. Subsequently, the volume CT dose index ($CTDI_{vol}$), the dose–length product (DLP), and the effective radiation dose equivalent (E) as obtained with use of automated anatomic tube current modulation were roughly estimated.

Based on the selected nominal tube current (mAs_{ref}) that was specified for each 64 MDCT examination, in addition the reference $CTDI_{vol}$, DLP, and effective dose (E) that would have been obtained without tube current modulation—that is, $CTDI_{vol\text{-}ref}$, DLP_{ref}, E_{ref}—were calculated using the same CT dose calculation software described above.

Statistical Analysis

All statistical analyses and graphs were performed with Sigma Stat 3.0 and Sigma Plot 8.0 (SPSS). Categoric variables are presented as a percentage and continuous variables (mAs, $CTDI_{vol}$, DLP, and radiation dose equivalent) are presented as mean and range or mean ± SD. A normality distribution test (Kolmogorov-Smirnov) was performed for all variables. Variables had Kolmogorov-Smirnov distribution between 0.029 and 0.136 ($p > 0.20$). A one-sample Student's t test was used to compare actual value to reference value for both 16- and 64-MDCT for each tube current voltage (80, 100, and 120 kV) for the following variables: tube current–time product (mAS), CTDI (mGy), DLP (mGy × cm), radiation dose (mSv), image quality (1–5), and image noise (H). In addition, a one-way analysis of variance with three factors (80 vs 100 vs 120 kVp) was used to compare the same variables across all three current voltages. If there was a significant effect between variables, the Scheffe post hoc test was performed to further specify the effects. A post hoc power analysis was not done because significant differences were found among variables in a one-way analysis of variance. A p value of 0.05 or less was considered to indicate a statistically significant difference for all statistical tests.

Tube current–time product, body weight, image quality, and image noise were treated as the dependent variables and the CT examination as the independent variable. Due to differences in tube voltage, CT examinations performed using 64-MDCT with automatic tube current modulation were further subdivided into 80-, 100-, and 120-kVp examinations. Because 64-MDCT examinations without automatic tube current modulation were only simulated (i.e., "virtual" examinations), patient body weight values are identical to 64-MDCT with automatic tube current modulation, and image quality scores and image noise levels, respectively, are not assessable. Any

associations for theses values, consequently, were established only for "true" examinations—that is, 64-MDCT with automatic tube current modulation and 16-MDCT, respectively. Because changes in $CTDI_{vol}$, DLP, and mean effective radiation dose (E_{mean}) are directly associated with changes of the tube current–time product, testing for statistical significance was defaulted to avoid data inflation.

All MDCT findings were compared with results of cardiac sonography, catheter angiography, and surgery. Agreement between methods was determined by using a binomial confidence interval for theta. Interobserver agreement was determined by correlating image quality scores and the detection rate of cardiovascular defects by means of Cohen's kappa statistic [26].

Results

Use of automated anatomic tube current modulation resulted in an average tube current–time product of 54.1 ± 44 mAs, a $CTDI_{vol}$ of 2.8 ± 3.1 mGy, and a DLP of 77.1 ± 103.7 mGy × cm, corresponding to an estimated mean effective radiation dose equivalent (E) of 2.5 ± 2.1 mSv (Table 2). In comparison with scanning without automated anatomic tube current modulation, the tube current–time product was significantly ($p < 0.05$) reduced by 57.8% (54.1 / 128.77 mAs). $CTDI_{vol}$ (–56.3%), DLP (–54.9%), and the radiation dose equivalent (E) (–60.3%) were reduced accordingly (Table 2). Because changes of these variables are directly associated with changes of the tube current–time product as outlined above, no testing for statistical significance was performed for these variables.

In comparison with 16-MDCT, 64-MDCT scanning with automatic tube current modulation resulted in a significant ($p < 0.05$) reduction of the tube current–time product (–26.3%; 54.1 / 104.37 mAs). $CTDI_{vol}$ (–61.5%), DLP (–40.3%), and the radiation dose equivalent (E) (–39.7%) were also markedly reduced (Table 3). Image quality scores and image noise levels were comparable for both CT scanners (Table 3 and Figs. 1 and 2).

Significant between-variable effects were observed for different tube voltages in 64-MDCT with automatic tube current modulation. Tube current–time product was significantly ($p < 0.05$) lower for 80-kVp scans than for 100- and 120-kVp scans but not for 100-kVp compared with 120-kVp scans (Table 4). This observation is a consequence of our study design: 80-kVp scanning was performed solely in patients weighing < 15 kg, who consequently were also scanned at a reduced tube current. $CTDI_{vol}$, DLP, and the radiation dose equivalent (E) were significantly ($p < 0.05$) higher for 120- than for 100- and 80-kVp scans, but not for 100-kVp compared with 80-kVp scans (Table 4). Mean CT image noise was 9.1 ± 2.9 H, showing no significant ($p = 1.0$) difference of means for different tube voltages (Table 4). Mean image quality was rated at 3.6 ± 0.4, also showing no significant ($p = 0.99$ and $p = 1.0$, respectively) influence by the level of tube voltage (Table 4 and Figs. 3 and 4).

All cardiovascular defects that had been documented on MDCT scans were correlated with findings at cardiac sonography. In the 38 patients, 59 defects had been observed using echocardiography. The difference in the number of defects and patients is explained by several patients having either had more than one cardiovascular defect or suffered from complex cardiovascular anomalies (e.g., tetralogy of Fallot, Klippel-Trénaunay-Weber syndrome, Ebstein's anomaly, and so on). Fifty-six cardiovascular defects were seen on MDCT scans by reviewer 1—corresponding to an agreement of 94.9% (95% CI, 85.8–98.9%)—and 54 by reviewer 2—corresponding to an agreement of 91.5% (95% CI, 81.3–97.1%). Reviewer 1 missed two atrial septal defects (ASDs) and one subvalvular stenosis, and reviewer 2 missed three ASDs, two pulmonary artery stenoses, and one subvalvular stenosis. In 31.6% of patients (12/38), CT scans were also correlated with surgery and in 23.7% of patients (9/38), with catheter angiography. Agreement with surgery was 100% (95% CI, 86.7–100%), and it was 100% (95% CI, 79.4–100%) with catheter angiography. Interobserver agreement was considered good with $\kappa = 0.76$ for quality scoring and $\kappa = 0.73$ for detection of cardiovascular defects.

TABLE 2: Radiation Exposure for 80- to 120-kV Scans: 64-MDCT with Automatic Tube Current Modulation (ATCM) in Comparison with Reference Values Estimated from Actual 64-MDCT mAs Values

Measure of Radiation Exposure	64-MDCT with ATCM			
	80 kVp (n = 17)	100 kVp (n = 9)	120 kVp (n = 12)	Mean
Tube current–time product (mAs)				
Actual value	24.8 ± 3.9	65.1 ± 45.9	76.7 ± 48	54.1 ± 44
Reference value[a]	72.3 ± 7.9	144.4 ± 70.3	174.2 ± 84.9	128 ± 77.5
Difference (%)	65.7	54.9	56.0	57.8
p	< 0.05	< 0.05	< 0.05	< 0.05
$CTDI_{vol}$ (mGy)				
Actual value	0.5 ± 0.1	2.2 ± 1.8	5.3 ± 3.2	2.8 ± 3.1
Reference valuea	1.5 ± 0.2	4.7 ± 2.4	12.2 ± 5.7	6.4 ± 6
Difference (%)	66.6	53.2	56.6	56.3
Dose–length product (mGy × cm)				
Actual value	8.5 ± 2.9	59.4 ± 50.9	156.8 ± 123.5	77.1 ± 103.7
Reference valuea	24.6 ± 8	128.1 ± 70.3	346.1 ± 220.2	171 ± 200.2
Difference (%)	65.4	53.6	54.7	54.9
Radiation dose equivalent (E) (mSv)				
Actual value	1.0 ± 0.2	1.9 ± 1.5	4.4 ± 2.1	2.5 ± 2.1
Reference value[a]	2.9 ± 0.7	4.5 ± 2.4	10.6 ± 3.7	6.3 ± 4.4
Difference (%)	65.5	57.8	58.5	60.3

[a]Values for 64-MDCT without ATCM were estimated from prevailing actual 64-MDCT mAs values.

Discussion

Evaluation of a sizable cohort of consecutive pediatric patients undergoing cardiovascular 64-MDCT shows that substantial reductions in radiation exposure can be realized by automated tube current modulation techniques without sacrificing diagnostic quality. Use of 120 kV for pediatric cardiovascular 64-MDCT incurs relatively higher radiation exposure but does not significantly improve diagnostic quality compared with CT acquisition with lower tube potential. Thus, lower tube voltage settings appear recommendable for this patient population.

TABLE 3: Radiation Exposure for 120-kVp Scans: 64-MDCT With Automatic Tube Current Modulation (ATCM) Compared with 16-MDCT Without ATCM

Parameter	64-MDCT With ATCM	16-MDCT Without ATCM[a]	Difference (%)	*p*
Tube current–time product (mAs)	104 ± 37.8	76.6 ± 48.0	26.3	< 0.05
$CTDI_{vol}$ (mGy)	13.8 ± 5.0	5.3 ± 3.2	61.5	NA
DLP (mGy × cm)	262.8 ± 125.7	156.8 ± 123.5	40.3	NA
Radiation dose equivalent (*E*) (mSv)	7.3 ± 2.8	4.4 ± 2.1	39.7	NA
Image quality (1–5)	3.6 ± 0.4	3.8 ± 0.3	5.5	0.97
Image noise (H)	8.9 ± 4.5	9.1 ± 2.8	2.2	0.31

Note—$CTDI_{vol}$ = volume CT dose index, DLP = dose–length product, NA = not available. Changes in CTDI, DLP, and *E* are directly associated with changes of the tube current–time product and thus testing for statistical significance was defaulted.
[a]Reference values derived from LightSpeed 16-MDCT scanner (GE Healthcare).

Reducing the tube current–time product as a function of patient size is a well-established method of reducing radiation exposure at CT [6–8, 13]. Automatic tube current modulation, a technique that adapts tube current on the basis of the size, shape, and geometry of the patient, is the most recent development in this realm [11, 18]. Initial results show significant dose savings in the range of 10–76% if this technique is used [9, 10, 17, 22, 27, 28]. We, as others [10, 28], found that compared with standard, nonmodulated scanning, diagnostic quality is not impaired and image noise is only slightly increased if automated tube current modulation is used. However, mean dose values of "virtual" 64-MDCT scans (i.e., simulated 64-MDCT scanning without automatic tube current modulation) were distinctly higher than those of "true" 16-MDCT examinations and thus point out a slight overestimation of actual dose savings when comparing actual 64-MDCT values to default reference values.

Beam energy (tube voltage) equally affects radiation exposure [13, 15, 29]. Huda et al. [30] showed that reducing the X-ray tube potential from 140 to 80 kVp at constant tube current can decrease the radiation dose by a factor of about 3.4. Image contrast and image noise will increase because there are fewer photons produced [29–31]. However, because the contrast-to-noise ratio (CNR) is the primary determinant of CT image quality, noise is rather irrelevant if the level of contrast is high enough and increases accordingly [32]. The change in image contrast is dependent on the anatomic number (*Z*) of the structures being investigated: image contrast of high-anatomic-number structures (e.g., vessels containing an iodinated contrast agent) becomes significantly more prominent at reduced tube voltages than image contrast of low-anatomic-number structures (e.g., soft tissue) [30].

In a phantom study, Siegel et al. [29] showed that reduced beam energy in contrast-enhanced pediatric CT decreases radiation dose without markedly affecting image contrast

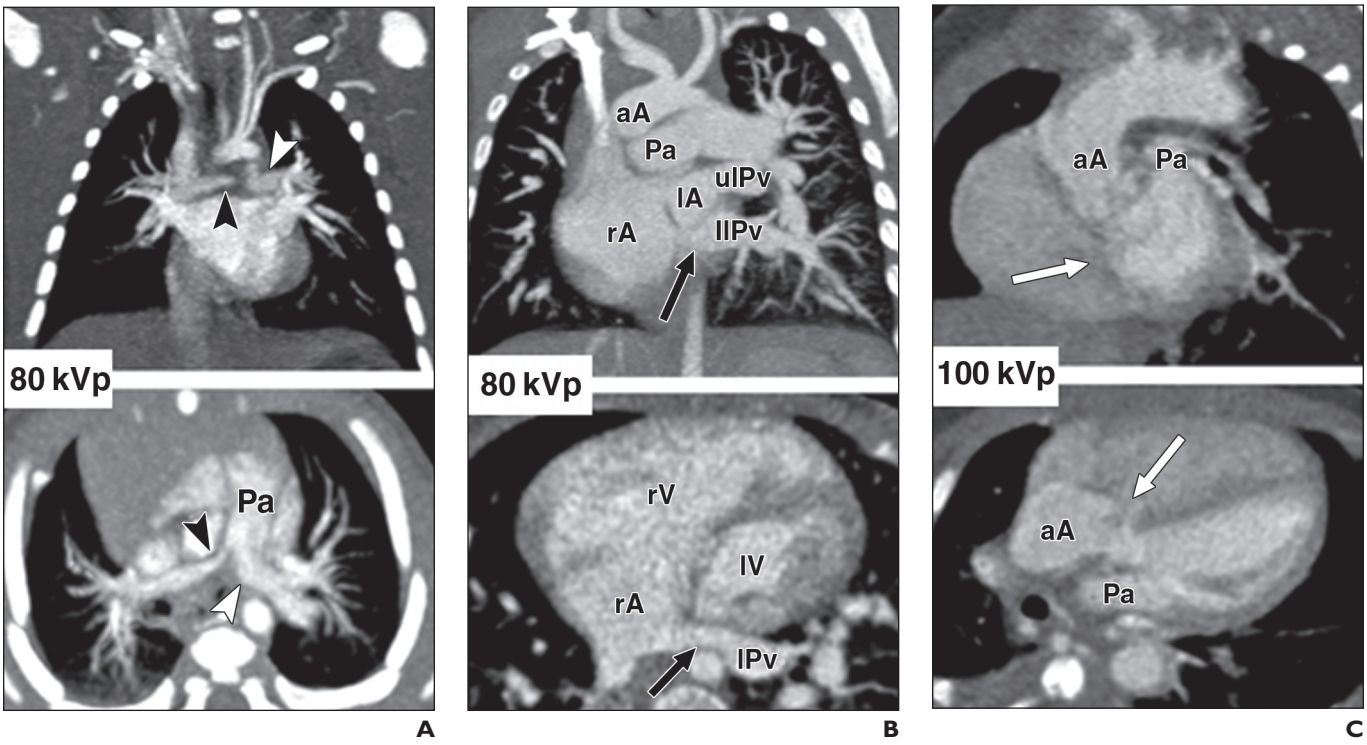

Fig. 1—Three different examples of congenital vascular abnormalities of chest evaluated with 64-MDCT with use of automatic tube current modulation.
A–C, Oblique coronal maximum-intensity-projection images (*upper row*) and transverse section images (*lower row*) of patients scanned at 80 kVp (**A** and **B**) and 100 kVp (**C**). **A** shows stenotic pulmonary artery (*black arrowheads*) in xx-year-old xxxxxx. Note difference in vessel caliber between right and left pulmonary arteries (*white arrowhead*). **B** shows left lower pulmonary vein (llPv) draining (*black arrows*) in right (rA) instead of left (lA) atrium in xx-year-old xxxxxx. ulPv = upper left pulmonary vein, rV = right ventricle, and lV = left ventricle. **C** shows tetralogy of Fallot with large septal defect (*white arrows*), overriding ascending aorta (aA), and stenotic pulmonary artery (Pa) in xx-year-old xxxxxx.

AQ-9

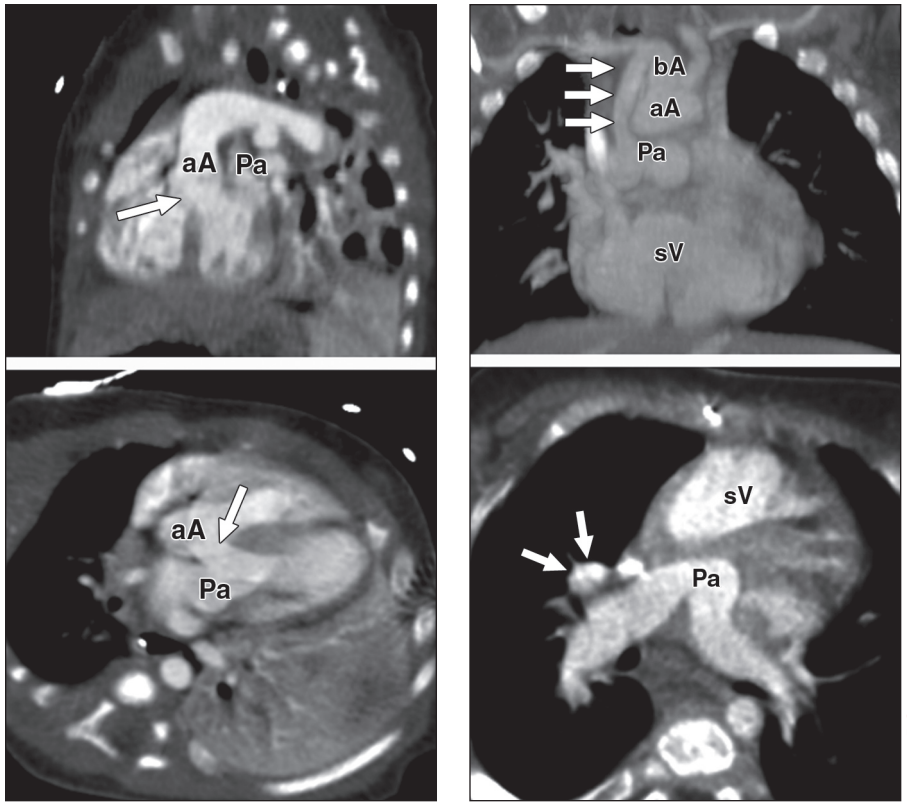

Fig. 2—Two examples of congenital vascular abnormalities of chest evaluated with 16-MDCT. **A** and **B,** Oblique sagittal multiplanar reformation images (*upper row left*), coronal maximum-intensity-projection images (*upper row right*), and transverse section images (*lower row*) of patients scanned at 120 kVp. **A** shows tetralogy of Fallot with large septal defect (*arrows*), overriding ascending aorta (aA), and stenotic pulmonary artery (Pa) in xx-year-old xxxxxx. Findings are similar to those in 64-MDCT (Fig. 3A). Image noise appears less for 16-MDCT images; however, differences were statistically not significant. **B** shows single ventricle (sV) after Blalock-Taussig shunt (*arrows*) between brachiocephalic (bA) and pulmonary (Pa) arteries in xx-year-old xxxxxx. AQ-9

TABLE 4: Radiation Exposure, Image Quality, and Image Noise for 80- to 120-kVp Scans

Parameter	Beam Energy (Tube Voltage)					
	80 vs 100 kVp		80 vs 120 kVp		100 vs 120 kVp	
	Difference of Means	*p*	Difference of Means	*p*	Difference of Means	*p*
Tube current–time product (mAs)	40.1	< 0.05	51.6	< 0.05	11.5	0.96
$CTDI_{vol}$ (mGy)	1.6	0.22	4.8	< 0.05	3.2	< 0.05
DLP (mGy × cm)	50.6	0.41	147.9	< 0.05	97.4	< 0.05
Radiation dose equivalent (*E*) (mSv)	0.9	0.81	3.4	< 0.05	2.5	< 0.05
Image quality (1–5)	0.08	1.0	–0.07	0.99	–0.08	1.0
Image noise (H)	–0.13	1.0	–0.10	1.0	–0.02	1.0

Note—$CTDI_{vol}$ = volume CT dose index, DLP = dose–length product.

and image noise. In the present study, significant differences in the effective radiation dose were observed for 120 kVp compared with 100- and 80-kVp scans, respectively, whereas image noise and quality scores were comparable. In pediatric patients ≥ 15 kg, beam energy of 100 kVp thus appears preferable over 120 kVp. However, reference dose values for different kV levels in the present study derive exclusively from "virtual" CT examinations and thus are of only limited valence. Unfortunately any perspective, intraindividual comparison of different scanning protocols that would be able to confirm our results appears ethically critical. AQ-2 AQ-4 AQ-5

In addition, the limited number of patients and the retrospective nature of our investigation did not allow the determination of suitable body–weight dependent cutoff values for different beam energies. Verdun et al. [15] proposed a cutoff value of 5 kg for 100 kVp and 30 kg for 120 kVp. Our preliminary data indicate that 80 kVp may easily be used for body weights of up to 15 kg and 100 kVp for up to 75 kg. However, Sigal-Cinqualbre et al. [23] reported good diagnostic image quality in patients up to 75 kg with 80-kVp scanning protocols, so the potential for dose reduction using low beam energies may not be fully exhausted.

The interrelationship between beam energy and tube output in terms of image noise has been described by Boone et al. [13], who characterized image noise for CT techniques using tube voltages of 80–140 kVp and tube currents of 10–300 mAs. Provided the tube current–time product was appropriately adapted, radiation dose was markedly reduced at lower tube voltage while CNR remained at a constant level. Cody et al. [33] reported that the use of 80-kVp tube voltage resulted in beam-hardening artifacts and thus recommended the use of 100- to 120-kVp settings in pediatric patients. Different from our investigation, their study was performed with 4 × 5 mm detector configuration using an axial (sequential) rather than helical acquisition mode and measuring only surface radiation. AQ-6

A limitation of our retrospective study is that radiation dose was not directly measured but calculated based on the DLP. However, as shown by Cohnen et al. [34], excellent correlation exists between effective dose and DLP measurements. The effective dose can be estimated by multiplying the appropriate conversion factor by the DLP [35]. However, determining pediatric radiation dose is less straightforward than in adults because the DLP is calculated on the basis of the $CTDI_{vol}$, and the U.S. Food and Drug Administration (FDA Center for Devices and Radiological Health) (CDRH) protocol for the measurement of $CTDI_{vol}$ is based on only two sizes of cylindric acrylic phantoms: 16 cm (simulating an adult's head) and 32 cm (simulating an adult's body). Phantom studies show that the mean imparted section dose increases with smaller patient diameter because there is less tissue absorbing radiation [13, 29, 31]. Thus

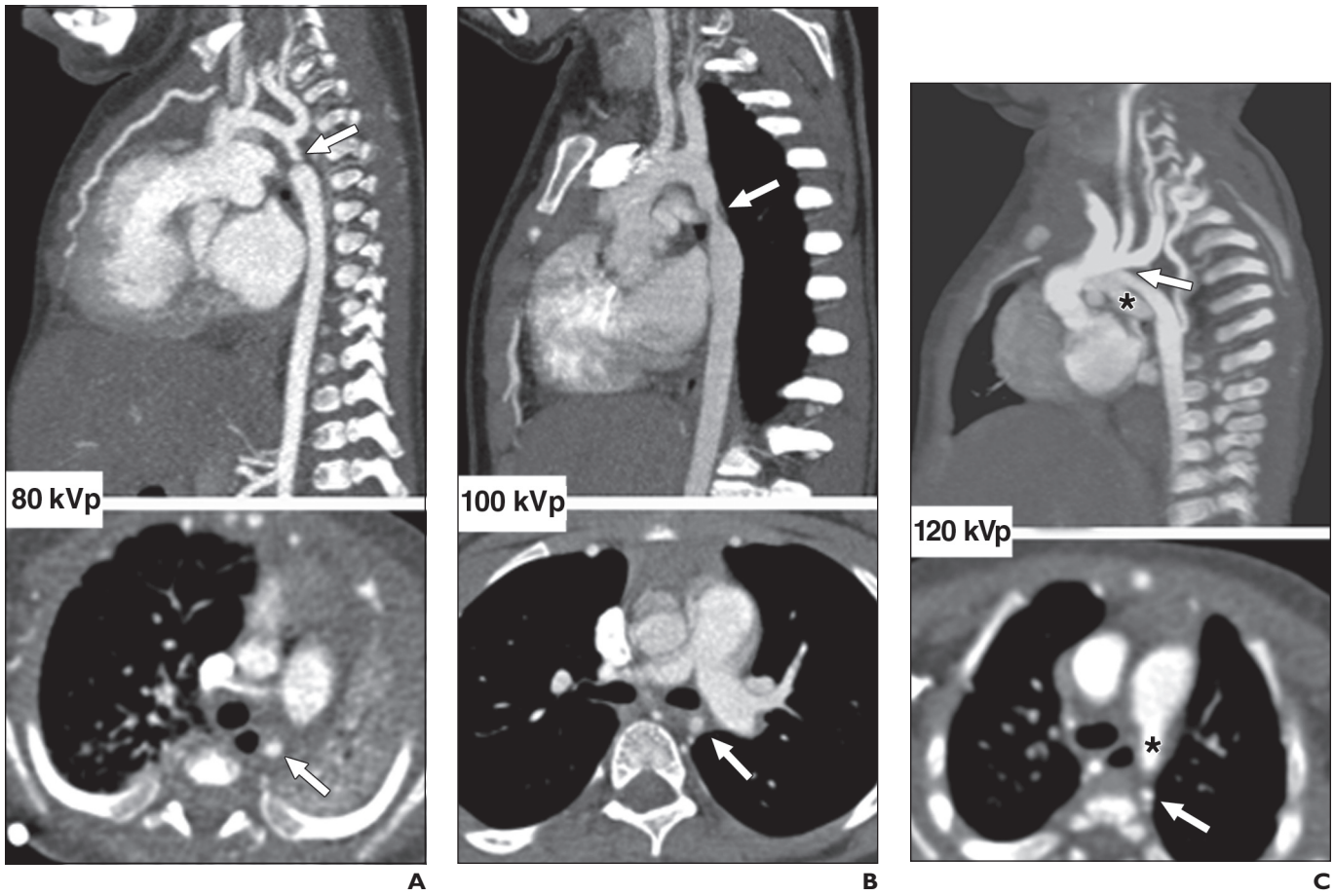

Fig. 3—Comparison of image quality and image noise in three patients with different types of congenital aortic arch abnormalities (*arrows*) evaluated with 64-MDCT with use of automatic tube current modulation.

A–C, Oblique sagittal maximum-intensity-projection images (*upper row*) and transverse section images (*lower row*) of patients scanned at 80 (**A**), 100 (**B**), and 120 (**C**) kVp appear grainier at lower compared with higher beam energy levels, but diagnostic quality is not compromised in any cases. Asterisk in **C** indicates patent ductus arteriosus in patient with an interrupted aortic arch.

AQ-10

children receive relatively more radiation than adults, whereas $CTDI_{vol}$ and DLP as indicated by the CT scanner remain the same [36]. We made allowance for this by using commercially available CT dose calculation software, which takes into consideration published age-dependent weighting factors for pediatric patients [25].

The influence of other scanning parameters, such as collimator thickness, pitch, and gantry cycle time, on radiation dose was not considered in the present study. Generally, thick sections and a relatively fast pitch reduce radiation dose in pediatric CT [5, 7, 16, 25, 37]. With the particular scanner used in our study, the tube current (mA) is automatically augmented if the pitch value is increased. Thus accelerating the pitch does not necessarily result in lower radiation [38]. As recommended by the FDA and to keep radiation dose as low as reasonably achievable (ALARA principle), we always use a fast gantry cycle time in children and design our scanning protocols with the goal of optimizing the pitch and tube current–time product relationship with regard to radiation dose [38].

Also, measurement of image noise levels is always critical because one cannot distinguish anatomic variability from CT-generated noise. However, we made allowance for this by also assessing subjective image quality perception by two independent readers and by choosing 64-MDCT and 16-MDCT examinations of patients with similar characteristics (body weight and age) (Table 1).

Another limitation is that noncooperative (breathing) and cooperative (nonbreathing) patients were not assessed separately in this study. Therefore, image quality may distinctly differ between both groups and thus influence our results. However, the number of patients appeared too small to further subdivide the groups without risking dilution of the statistical information. In addition, the aim of the study was not to compare image quality of different groups or scanners but to show that no differences were found in this set of subjects.

Finally, any comparison between scanners of different manufacturers has limitations. In particular, direct comparison of mAs values of different scanners is critical because the effect on image quality and patient dose differs from scanner to scanner. However, we tried to account for these limitations by introducing objective measurement criteria such as image noise and by calculating approximated tube current levels for scanning without automatic tube current modulation on the basis of the selected nominal tube current that was specified for each 64-MDCT examination. It would certainly be preferable to compare scanning without automatic tube current modulation to scanning with automatic tube current modulation

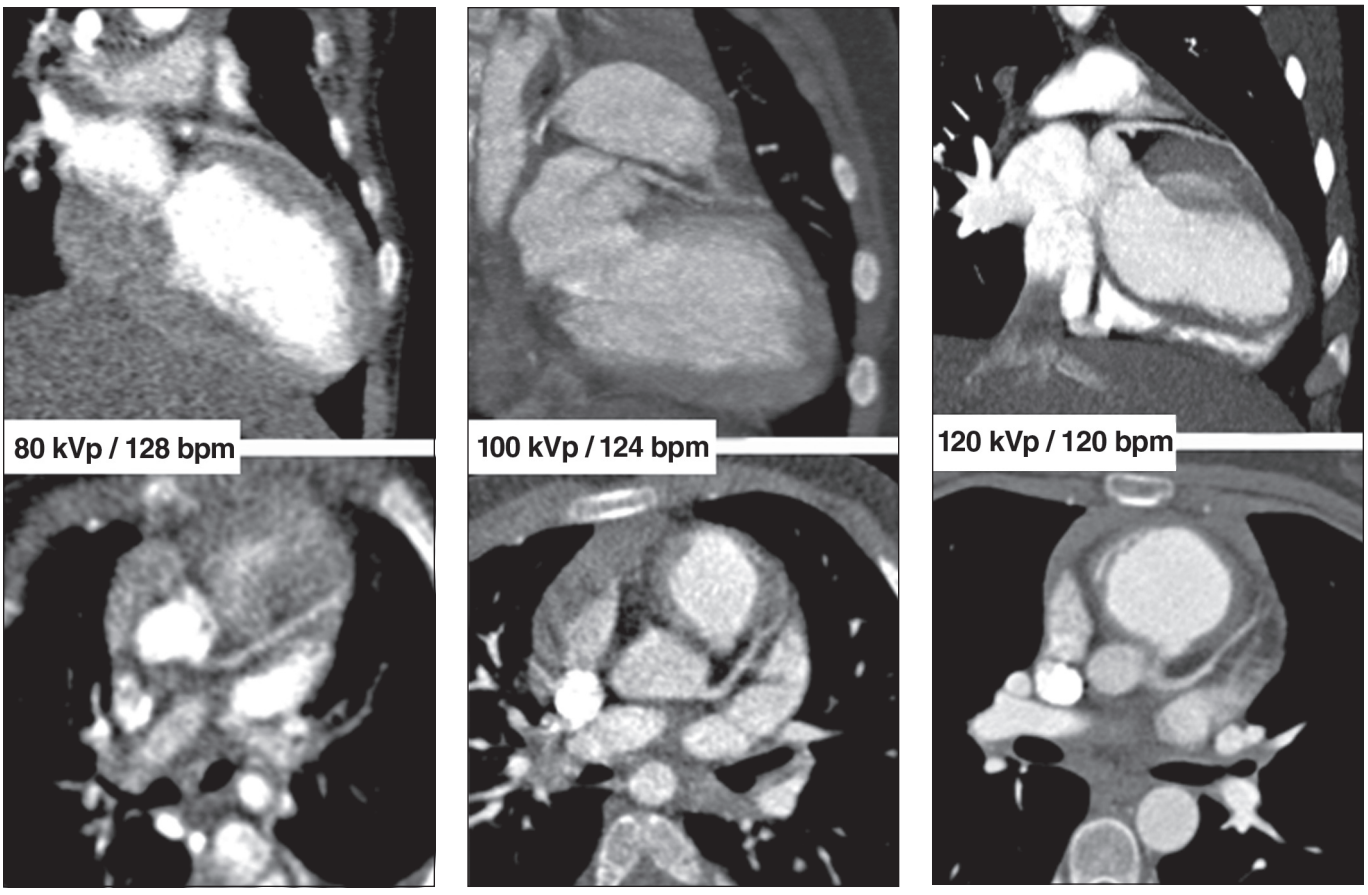

Fig. 4—Examples of image quality obtained at level of aortic root with 64-MDCT and use of automatic tube current modulation.
A–C, Oblique sagittal minimum-intensity-projection images (*upper row*) and transverse sections (*lower row*) of patients scanned at 80 (**A**), 100 (**B**), and120 (**C**) kVp. To reduce radiation exposure all patients were scanned in free-breathing technique and without use of ECG gating. Nevertheless, in most cases, ascending aorta and origin of coronary arteries were deemed of diagnostic (grading score > 3) image quality. Note only minimal motion artifacts in myocardium. bpm = beats per minute.

AQ-10

in the same patient or at least on the same scanner. However, to tolerate this in children solely for study purposes appears unethical. In the end, the aim of the study was not to show superiority of scanning with automatic tube current modulation over scanning without automatic tube current modulation but to show that this technique provides sufficient image quality at distinctly reduced tube-current levels.

In conclusion, in pediatric cardiovascular CT of the chest, automated tube current modulation combined with low tube voltage leads to significantly decreased radiation dose while image quality is maintained. Standard tube potentials as they are used in adults tend to increase radiation in children without significantly improving image quality.

References

1. Committee to Assess Health Risks from Exposure to Low Levels of Ionizing Radiation, National Research Council. *BEIR VII: health risks from exposure to low levels of ionizing radiation.* Washington, DC: The National Academies Press, 2005. fermat.nap.edu/openbook/030909156X/html/index.html. Accessed xxxxxxxxxx

AQ-7

2. Brenner DJ, Elliston CD, Hall EJ, Berdon WE. Estimates of the cancer risks from pediatric CT radiation are not merely theoretical: comment on "point/counterpoint: in x-ray computed tomography, technique factors should be selected appropriate to patient size—against the proposition." (commentary) *Med Phys* 2001; 28:2387–2388
3. Brenner DJ. Estimating cancer risks from pediatric CT: going from the qualitative to the quantitative. *Pediatr Radiol* 2002; 32:228–231
4. Mettler FA, Wiest PW, Locken JA. CT scanning: patterns of use and dose. *J Radiol Prot* 2000; 20:353–359
5. Linton OW, Mettler FA Jr. National Conference on Dose Reduction in CT, with an emphasis on pediatric patients. *AJR* 2003; 181:321–329
6. Kamel IR, Hernandez RJ, Martin JE, Schlesinger AE, Niklason LT, Guire KE. Radiation dose reduction in CT of the pediatric pelvis. *Radiology* 1994; 190:683–687
7. Brody AS. Thoracic CT technique in children. *J Thorac Imaging* 2001; 16:259–268
8. Lucaya J, Piqueras J, Garcia-Pena P, Enriquez G, Garcia-Macias M, Sotil J. Low-dose high-resolution CT of the chest in children and young adults: dose, cooperation, artifact incidence, and image quality. *AJR* 2000; 175:985–992
9. Kalra MK, Maher MM, Kamath RS, et al. Sixteen-detector row CT of abdomen and pelvis: study for optimization of *z*-axis modulation technique performed in 153 patients. *Radiology* 2004; 233:241–249
10. Kalra MK, Maher MM, Toth TL, Kamath RS, Halpern EF, Saini S. Comparison of *z*-axis automatic tube current modulation technique with fixed tube current CT scanning of abdomen and pelvis. *Radiology* 2004; 232:347–353
11. Kalra MK, Maher MM, Toth TL, et al. Techniques and applications of automatic tube current modulation for CT. *Radiology* 2004; 233:649–657
12. Flohr T, Stierstorfer K, Raupach R, Ulzheimer S, Bruder H. Performance evaluation of a 64-slice CT system with z-flying focal spot. *Rofo* 2004;

176:1803–1810
13. Boone JM, Geraghty EM, Seibert JA, Wootton-Gorges SL. Dose reduction in pediatric CT: a rational approach. *Radiology* 2003; 228:352–360
14. Das M, Mahnken AH, Mühlenbruch G, et al. Individually adapted examination protocols for reduction of radiation exposure for 16-MDCT chest examinations. *AJR* 2005; 184:1437–1443
15. Verdun FR, Lepori D, Monnin P, Valley JF, Schnyder P, Gudinchet F. Management of patient dose and image noise in routine pediatric CT abdominal examinations. *Eur Radiol* 2004; 14:835–841
16. Honnef D, Wildberger JE, Stargardt A, et al. Multislice spiral CT (MSCT) in pediatric radiology: dose reduction for chest and abdomen examinations [in German]. *Rofo* 2004; 176:1021–1030
17. Gies M, Kalender WA, Wolf H, Suess C. Dose reduction in CT by anatomically adapted tube current modulation. Part I. Simulation studies. *Med Phys* 1999; 26:2235–2247
18. Kalender WA, Wolf H, Suess C, Gies M, Greess H, Bautz WA. Dose reduction in CT by on-line tube current control: principles and validation on phantoms and cadavers. *Eur Radiol* 1999; 9:323–328
19. Mayo JR, Aldrich J, Muller NL. Radiation exposure at chest CT: a statement of the Fleischner Society. *Radiology* 2003; 228:15–21
20. Irie T, Inoue H. Individual modulation of the tube current-seconds to achieve similar levels of image noise in contrast-enhanced abdominal CT. *AJR* 2005; 184:1514–1518
21. Sprawls PJ. AAPM tutorial: CT image detail and noise. *RadioGraphics* 1992; 12:1041–1046
22. Kalra MK, Maher MM, D'Souza RV, et al. Detection of urinary tract stones at low-radiation-dose CT with z-axis automatic tube current modulation: phantom and clinical studies. *Radiology* 2005; 235:523–529
23. Sigal-Cinqualbre AB, Hennequin R, Abada HT, Chen X, Paul JF. Low-kilovoltage multi-detector row chest CT in adults: feasibility and effect on image quality and iodine dose. *Radiology* 2004; 231:169–174
24. Bongartz G, Golding SJ, Jurik AG, Leonardi M, van Meerten EvP. *European guidelines on quality criteria for computed tomography 1998*. Brussels, Belgium: European Commission, 1998. www.drs.dk/guidelines/ct/quality. Accessed xxxxxxxx.
25. Shrimpton PC, Wall BF. Reference doses for pediatric computed tomography. *Radiat Prot Dosim* 2000; 90:249–252
26. Cohen J. A coefficient of agreement for nominal scales. *Educ Psych Meas* 1960; 20:37–46
27. Greess H, Nömayr A, Wolf H, et al. Dose reduction in CT examination of children by an attenuation-based on-line modulation of tube current (CARE Dose). *Eur Radiol* 2002; 12:1571–1576
28. Greess H, Lutze J, Nömayr A, et al. Dose reduction in subsecond multislice spiral CT examination of children by online tube current modulation. *Eur Radiol* 2004; 14:995–999
29. Siegel MJ, Schmidt B, Bradley D, Suess C, Hildebolt C. Radiation dose and image quality in pediatric CT: effect of technical factors and phantom size and shape. *Radiology* 2004; 233:515–522
30. Huda W, Scalzetti EM, Levin G. Technique factors and image quality as functions of patient weight at abdominal CT. *Radiology* 2000; 217:430–435
31. Nickoloff EL, Alderson PO. Radiation exposures to patients from CT: reality, public perception, and policy. *AJR* 2001; 177:285–287
32. Huda W. Dose and image quality in CT. *Pediatr Radiol* 2002; 32:709–713
33. Cody DD, Moxley DM, Krugh KT, O'Daniel JC, Wagner LK, Eftekhari F. Strategies for formulating appropriate MDCT techniques when imaging the chest, abdomen, and pelvis in pediatric patients. *AJR* 2004; 182:849–859
34. Cohnen M, Poll LJ, Puettmann C, Ewen K, Saleh A, Mödder U. Effective doses in standard protocols for multi-slice CT scanning. *Eur Radiol* 2003; 13:1148–1153
35. Jessen KA, Shrimpton PC, Geleijns J, Panzer W, Tosi G. Dosimetry for optimization of patient protection in computed tomography. *Appl Radiat Isot* 1999; 50:165–172
36. Huda W, Atherton JV, Ware DE, Cumming WA. An approach for the estimation of effective radiation dose at CT in pediatric patients. *Radiology* 1997; 203:417–422
37. Paterson A, Frush DP, Donnelly LF. Helical CT of the body: are settings adjusted for pediatric patients? *AJR* 2001; 176:297–301
38. Feigal DWJ. Public health notification: reducing radiation risk from computed tomography for pediatric and small adult patients. Center for Devices and Radiological Health (CDRH), Food and Drug Administration Website, 2001. www.fda.gov/cdrh/safety/110201-ct.html. Accessed xxxxxxxxxxxxx